Environmental Science & Technology

pubs.acs.org/est

Article

Watching Paint Dry: Organic Vapor Emissions from Architectural Coatings and their Impact on Secondary Organic Aerosol Formation

Rebecca Tanzer-Gruener, Pavithra Ethi Rajan, Liam D. Dugan, Mark E. Bier, Allen L. Robinson, and Albert A. Presto*

Cite This: https://doi.org/10.1021/acs.est.2c02478

Read Online

ACCESS | Metrics & More | Article Recommendations | Supporting Information

ABSTRACT: Emissions from volatile chemical products (VCPs) are emerging as a major source of anthropogenic secondary organic aerosol (SOA) precursors. Paints and coatings are an important class of VCPs that emit both volatile and intermediate volatility organic compounds (VOCs and IVOCs). In this study, we directly measured I/VOC emissions from representative water- (latex) and oil-based paints used in the U.S. Paint I/VOC emissions vary by several orders of magnitude by both the solvent and gloss level. Oil-based paints had the highest emissions (>10^5 μg/g-paint), whereas low-gloss interior paints (Flat, Satin, and Semigloss) all emitted ~10^2 μg/g-paint. Emissions from interior paints are dominated by VOCs, whereas exterior-use paints emitted a larger fraction of IVOCs. Extended emission tests showed that most I/VOC emissions occur within 12−24 h after paint application, though some paints continue to emit IVOCs for 48 h or more. We used our data to estimate paint I/VOC emissions and the subsequent SOA production in the U.S. Total annual paint I/VOC emissions are 48−155 Gg (0.15−0.48 kg/person). These emissions contribute to the formation of 2.2−7.5 Gg of SOA annually. Oil-based paints contribute 70−98% of I/VOC emissions and 61−99% of SOA formation, even though they only account for a minority of paint usage.

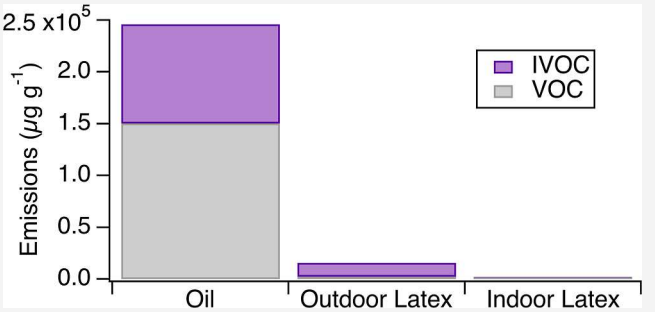

KEYWORDS: *emissions, VCP, volatility, PTR-MS, paint, urban*

1. INTRODUCTION

$PM_{2.5}$, particulate matter with a diameter of less than 2.5 μm, has deleterious effects on human health and the environment.[1,2] Exposure to elevated concentrations of $PM_{2.5}$ is associated with increased risk of respiratory and cardiovascular diseases, making poor air quality one of the leading preventable causes of death worldwide.[3]

A significant portion of the $PM_{2.5}$ mass (20−90%) is organic aerosol (OA). OA is classified as either primary (POA) or secondary (SOA).[4] SOA forms through reactions in the atmosphere and makes up a significant portion of ambient OA even in urban areas.[5−8] SOA is formed when pollutants which are emitted as vapors such as volatile organic compounds (VOCs) react with oxidants, and the subsequent products condense into the particle phase. Here, we define VOCs as organic compounds with effective saturation concentrations (C*) greater than 3.2 × 10^6 μg/m^3. Less volatile organics such as intermediate volatile organic compounds (IVOCs, 3.2 × 10^6 ≥ C* ≥ 3.2 × 10^2 μg/m^3) also can be important SOA precursors,[9−11] potentially contributing as much as 50% of urban SOA.[12]

Historically, mobile sources have been a large source of anthropogenic SOA precursors. However, as vehicles have become cleaner due to regulations and new technologies,[13] the importance of SOA formation from emissions from non-combustion sources such as volatile chemical products (VCPs) has increased.[14,15] VCPs contribute about a quarter of VOC emissions in the U.S.; this is similar to mobile source emissions from diesel and gasoline vehicles.[14] The majority of research on anthropogenic sources of SOA has focused on emissions from combustion processes,[16−18] despite the fact that VCPs are thought to have significant SOA yields.[19] In order to address this gap, we need to quantify the magnitude and composition of SOA-forming emissions from VCPs.

One challenge for understanding emissions from VCPs is that these products cover a wide range of forms and functions including cleaning supplies, personal care products, paints and coatings, and many other products. Emissions from some of these products are more atmospherically relevant than others due to their timescales and modes of emission. Paints and coatings, which made up 13% of the U.S. organic solvent

Received: April 8, 2022
Revised: July 18, 2022
Accepted: July 19, 2022

consumption for 2012, are thought to contribute to significant VOC emissions.[14,15] Seltzer et al. recently estimated that paints and coatings contribute 33% of VCP and VOC emissions in the United States, with architectural coatings contributing 21% of the paint sector emissions.[20]

Although many previous studies have characterized paint emissions,[21−25] there has been little effort to understand their contribution to SOA formation. For example previous studies have quantified emissions of hazardous VOCs,[24,26,27] emissions of individual VOCs,[28−30] their impact on indoor air quality,[31] and their outdoor ozone reactivity.[32] However, we are not aware of any published experimental work that has quantified I/VOC (IVOC + VOC) emissions from paints and their contribution to SOA formation.

This paper describes experimental measurements of I/VOC emissions from a range of different paints. We use these data to estimate the contribution of architectural coatings to I/VOC concentrations and SOA formation potential in the U.S.

2. INSTRUMENTATION AND METHODS

2.1. Materials. The paint sector is very large. Under the U.S. Census Bureau's classification of "architectural coatings" (category#: 3255101), the mass of architectural paints used per year, scaled to the 2021 population, is 3.1 Tg.[33] Architectural coatings make up 59% of the total paint usage in the U.S., with the remainder dominated by industrial coatings.[20]

Variability across the large architectural coating sector stems from differences in the solvent (water vs oil), manufacturer, gloss level (high through low), indoor versus outdoor use, and the presence of different binders and pigments; all of these factors can impact emissions.[34] One of the major differentiators between paints is whether they are oil- (alkyd) or water- (acrylic/latex) based. Fifty years ago, most paints were oil-based because of their resistance to wear and ease of application.[35] However, oil-based paints contain much higher levels of VOCs, and over the past few decades, there has been a dramatic shift to water-based paints.[35] In general, water-based paints have <250 g/L of VOCs, while oil-based paints are required to have <380 g/L of VOCs.[36] There are also "low-VOC" paints which are required to have <5 g/L of VOCs. These requirements apply only to the organic solvent portion of the paints and do not account for "exempt" VOCs or water. Some VOCs, including acetone, are classified as exempt VOCs by both the U.S. EPA and the California Air Resources Board (CARB) because of their low ozone formation potential. Thus, while these exempt VOCs fit the traditional definition of a VOC based on vapor pressure, they do not meet the regulatory definition of a VOC present in consumer products.

Our approach was to sample as broad an array of architectural coatings as possible. The U.S. Census Bureau inventory[33] includes 23 classifications of paints which can be grouped into five categories of latex paint (Flat, Semi-gloss Interior [SemiInt], Semi-gloss Exterior [SemiExt], High Gloss, and Satin) and oil-based paint. We tested commercially available paints from each of these categories. A full description of the paints selected can be found in Table S1 in the Supporting Information.

2.2. Procedures. We conducted two types of experiments with each paint: (1) headspace sample and (2) extended emission experiments. These experiment types are described in detail below, with additional details available in Section S1 of the Supporting Information. All experiments were conducted at 22 ± 2 °C.

The extended emission experiments quantified the total mass of I/VOC emissions for 48 h after paint application. Extended emission experiments were conducted in two different flux chambers. Most experiments used a 1.2 L aluminum flux chamber (Figure S1), while others used a larger 23 L fiberglass flux chamber. At the start of each extended emission experiment, a piece of the pre-cut substrate was weighed, painted (~58 cm^2 painted surface), re-weighed to determine the mass of the paint applied, and immediately placed into the chamber. As shown in Table S2, most experiments used ~1−2 g of paint. The chamber was then sealed, and sampling began. Activated-carbon-filtered air was pulled through the flux chamber at a flowrate of 0.37 slpm. This gave a residence time of 3.2 min (air exchange rate of 18.75 h^{-1}) for the aluminum chamber and 62 min (air exchange rate of 0.96 h^{-1}) for the fiberglass chamber.

The total mass emissions were computed via mass balance: $\dot{E}_i = \Delta C_i Q$, where $\dot{E}_i$ (μg/s) is the mass emission rate of species i, ΔC_i is the background-corrected concentration of species i ($\mu g/m^3$), and Q is the flow rate of air through the flux chamber (m^3/s). The background-corrected concentration is determined by collecting a blank sample from the empty flux chamber before the start of each experiment. The total emission per mass of paint (μg/g-paint) is determined by integrating $\dot{E}$ for each species over the entirety of the experiment and dividing by the mass of paint used.

Most extended emission experiments used drywall as a substrate as it is a commonly painted surface material throughout the United States. Several experiments, primarily with outdoor use paints, were also conducted with wood and metal as the substrate (Table S2).

Headspace experiments were used to obtain a fingerprint of paint vapors. In these experiments, we sampled directly (~5 cm) above open paint cans that were placed in a fume hood. Figure S1 shows a schematic of the headspace experimental setup.

We used multiple methods to comprehensively quantify the composition of paint I/VOCs in both the headspace and extended emission experiments. VOCs and more volatile IVOCs (e.g., naphthalene) were measured with quadrupole proton transfer reaction mass spectrometry (PTR-MS).[37] The proton transfer reaction mass spectrometer was operated in scan mode from m/z 21 to 155 and sampled continuously for the entirety of the extended emission tests (typically 48 h).

IVOCs were primarily quantified using Tenax sorbent tubes, followed by thermal desorption GC−MS gas chromatography−mass spectrometry (GC−MS) analysis. Tenax TA was selected as the sorbent material because it performs well while sampling in high moisture environments and is known to be effective at measuring I/VOCs.[38−40] A full description of the GC−MS system, sorbent tube cleaning, and analysis procedures can be found in section S1.3 in the Supporting Information.

Tenax tube samples were collected over one-hour intervals,0−1, 1−2, 4−5, 8−9, 24, and 48 h, after paint application. Table S2 in the Supporting Information shows the exact sampling times for each experiment.

2.3. Analysis and Compound Identification. To estimate the SOA formation potential of paint emissions, we need to quantify the I/VOC emissions by both volatility (C*, $\mu g/m^3$) and composition. We did this by combining data from PTR-MS and GC−MS to comprehensively characterize the

https://doi.org/10.1021/acs.est.2c02478
Environ. Sci. Technol. XXXX, XXX, XXX−XXX

total I/VOC emission per mass of paint applied for all six of the tested paint types.

A challenge is that the complexity of paint emissions makes them hard to speciate at the molecular level. For example, IVOCs captured on the Tenax sorbent tubes cannot be fully speciated using one-dimensional GC. Instead, most of the GC signal appears as an unresolved complex mixture (UCM). An example chromatograph is shown in Figure 1a. There are few well-defined peaks. Instead, most of the mass elutes as a broad UCM hump. Since SOA formation depends on volatility and molecular structure,[41,42] one must quantify the total mass of emissions with enough chemical specificity to estimate SOA yields.

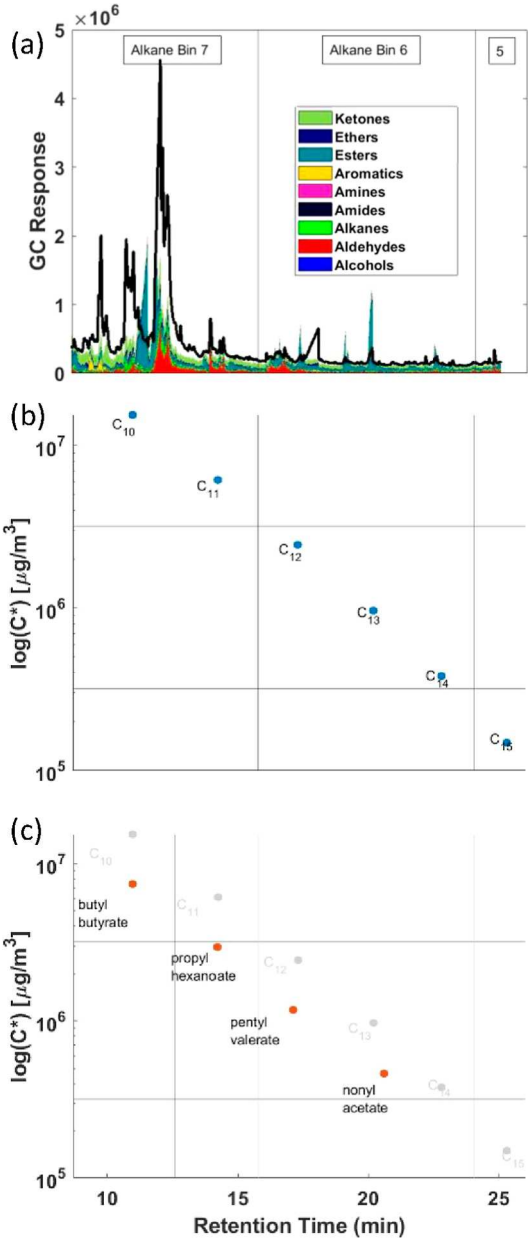

Figure 1. Volatility binning and compound class grouping. (a) Total ion chromatograph of a Satin paint headspace sample is shown by the thick black line. The signal decomposed into compound class contributions using marker ions is shown with the color shading. Vertical lines show logarithmically spaced C* bins determined from the alkane retention time and volatility (e.g., alkane bin 7 corresponds to the C* = 10^7 μg/m^3 bin). The relationship between the retention time and volatility is shown for a series of n-alkanes (b) and esters (c). (c) also shows the alkanes as light points to highlight the offset in ester volatility, relative to alkanes.

2.3.1. Analysis of GC−MS Data. We aim to characterize the total mass, volatility, and the chemical nature of the UCM. We use GC elution time to characterize volatility and the mass spectral data to characterize the chemical composition. Previous work has used GC−MS analysis to quantify UCM emissions from combustion systems.[43,44] We draw and expand these methods here; additional details are provided in Section S1.3 of the Supporting Information.

Previous work has used the retention time−volatility relationship to map the UCM to the volatility basis set for combustion emissions.[45,46] An example of this binning is shown in Figure 1b for a homologous series of *n*-alkanes. There is a nearly linear relationship between log(C*) and retention time. This relationship can in turn be used to classify UCM into logarithmically spaced C* bins, which are shown as vertical lines in Figure 1a,b.

IVOC emissions from combustion systems are generally dominated by aliphatic and aromatic hydrocarbons.[47] Since variations in hydrocarbon volatility are mostly a function of the carbon number (rather than molecular structure),[48] in previous work, a single relationship between retention time and volatility has been sufficient. However, paint emissions contain other, often more polar, compound classes (e.g., ketones, aldehydes, alcohols, and esters) that may have different relationships between C* and retention time. Therefore, mapping the GC−MS signal into C* bins requires classifying the UCM by composition.

An example of a different C*-retention time relationship is shown for a series of esters in Figure 1c. While retention time and C* show a log-linear relationship for the esters, the esters are offset relative to the alkanes. This means that we cannot use the C* bins defined by alkane retention times for the esters; hence, Figure 1c shows different boundaries for the C* bins for esters. Thus, to bin the UCM mass emitted from the paints, we need to separately quantify volatility for each compound class of interest. We calibrated the C*-retention time relationship for nine classes of compounds (alcohols, aldehydes, alkanes, amides, amines, aromatics, esters, ethers, and ketones) and defined separate retention time windows for each C* bin. Full details are presented in Table S3.

Since the relationship between C* and retention time varies by the compound class, mapping the UCM volatility also requires apportioning the GC signal into the nine compound classes shown in Figure 1a. This was done using marker ions in the mass spectra. We identified marker ions using two basic rules: (1) the marker needed to be unique or nearly unique to the compound class of interest and (2) the marker ion needed to make up a non-trivial amount (ideally >5%) of the overall signal for the compound class.

While there are common marker ions routinely used to interpret mass spectra,[49] they are not necessarily appropriate for use in our analysis, given the complexity of the signal. For example, *m/z* 57 is a common marker ion for hydrocarbons, but it is a poor marker ion for our samples because *m/z* 57 appears in the mass spectrum for nearly every molecule with a long carbon chain. Therefore, it is not specific enough to use as a marker ion for paint analysis. Instead, we used the NIST (National Institute of Standards and Technology) mass spectral library to determine marker ions for each of our

https://doi.org/10.1021/acs.est.2c02478
Environ. Sci. Technol. XXXX, XXX, XXX−XXX

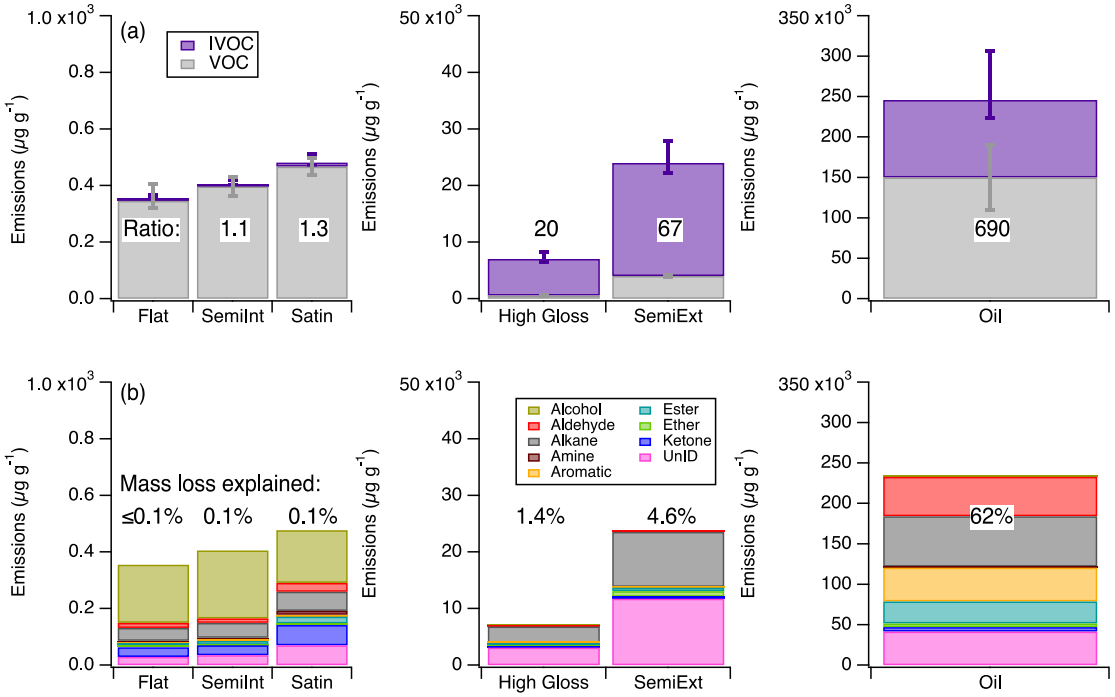

Figure 2. Total I/VOC emissions (μg/g-paint) over two-day extended emission experiments. Panel (a) separates the emissions into IVOC and VOC, and (b) separates by the compound class. Error bars in panel (a) show the full range of experiment-to-experiment variability for VOCs and the uncertainty associated with UCM apportionment for IVOCs, as described in SI section S2. Numbers in panel (a) show the ratio of the total I/VOC emissions to the emissions for Flat paint, which had the lowest emissions. Numbers in panel (b) show the mass fraction of emissions explained by measured I/VOCs.

nine compound classes. Table S4 shows the selected marker ions for each compound class and the contribution of that ion to the total ion signal, as determined from the NIST mass spectral library. Example mass spectra showing marker ion selection are shown in Figure S2.

The GC−MS signal was thus classified by both the compound class and volatility. We first extracted the marker ion signals from the total ion chromatogram and scaled them by the corresponding volatility-dependent multiplier from Table S4. This scaled signal was subsequently converted to mass, using calibrations from authentic standards of the compound class and volatility bin specific representative compounds (Table S3). All GC−MS samples were also corrected for recovery of a deuterated internal standard (Section S1.3). Volatility was then apportioned using the predefined volatility bins described above. The net result of this analysis is shown in Figure 1a, where the colors indicate contribution of different compound classes. Any unapportioned signal (the white area in Figure 1a) was assumed to have the same volatility relationship and mass calibration as alkanes. GC−MS data for the headspace samples of each paint type are shown in Figure S3. Section S2 in the SI provides additional discussion on uncertainty in quantifying the UCM.

2.3.2. Analysis of PTR-MS Data. Our PTR-MS has unit mass resolution. It therefore is unable to separate isobaric ions, nor can it distinguish between compounds with the same elemental composition. We addressed this in several ways, as detailed below. Compound assignments are shown in Table S5 of the SI.

For most mass fragments, compound identification relied on the PTR-MS library[30] to identify possible compounds for a given mass-to-charge ratio (m/z). One exception was m/z 45. This ion is traditionally identified as acetaldehyde, but it has been suggested that it is likely ethylene glycol in paint emissions.[23]

For some m/z values, there is only one suggested compound in the PTR-MS library; however, there are many others which may have contributions from multiple compounds. For those m/z values, a search on PubChem was conducted to identify the most likely of the suggested compounds to be found in paints.

Not all m/z values that were detected in PTR-MS were able to be identified with the combination of the PTR-MS library and PubChem. To further aid in the identification, an open headspace analysis of each paint sample was conducted with the high resolution ThermoFisher Scientific Exactive Plus extended mass range (EMR) mass spectrometer. The orbitrap, operated in the normal mass range, allowed for exact mass measurements using a resolution of 140 000 at m/z 200. A custom atmospheric pressure chemical ionization (APCI) setup operated at 1400 V was used to generate the ions from the paint emissions. According to the orbitrap instrument manual, the external calibration, which was performed prior to acquisition, is expected to provide a <3 ppm mass accuracy. To further improve the ppm mass accuracy of detected species, a lock mass calibration technique that utilized a persistent background peak as the lock mass was introduced. To select a proper peak, caffeine, a common mass spectrometry standard with a monoisotopic ion mass of m/z 195.08765 first served as a lock mass to determine the exact mass of the background peak. A closely neighboring persistent background peak at 195.17421 amu was found and was then selected to serve as the lock mass for all the analyses. After acquisition, the elemental composition tool in XCalibur 4.1 (ThermoFisher Scientific, San Jose, CA, USA) was used to find the best

https://doi.org/10.1021/acs.est.2c02478
Environ. Sci. Technol. XXXX, XXX, XXX−XXX

matching chemical formulas based on the elements C, H, N, O, P, and S for the selected chemical species.

The orbitrap data allowed us to better constrain isobaric species that could not be separated by PTR-MS. It also enabled us to identify several fragment ions of texanol (2,2,4-trimethyl-1,3-pentanediol monoisobutyrate), an ester found in many latex paints. These fragments occur at m/z 69, 89, 111, and 129. Ions at these m/z are commonly assigned to other species when detected with PTR-MS, for example, isoprene or cyclopentene at m/z 69, hydroxyphenol at m/z 111, and naphthalene at m/z 129. Since texanol is a latex paint additive, we attribute these ions to texanol for the latex paints, but not for the oil-based paint. Stockwell et al.[23] previously assigned m/z 111 and 129 to texanol fragments for water-based paints. Table S5 shows a full list of ions scanned by PTR-MS, the compound assigned to that m/z, and the resources used to make that determination (PTR library, PubChem, and/or APCI Orbitrap).

Following our comprehensive identification of compounds measured by PTR-MS, with the help of the EMR measurements, the emissions were also classified into one of the nine compound groups used in the GC−MS analysis. Effective saturation concentrations (C*) were calculated for individual compounds using the SIMPOL method[48] and from GC retention times for the UCM to classify the compounds as either IVOCs or VOCs. SIMPOL typically estimates C* within a factor of two. Ultimately, masses of I/VOCs measured by both GC−MS and PTR-MS were added together to obtain the total I/VOC emissions per mass of paint applied (μg/g) for the tested paint types.

3. RESULTS AND DISCUSSION

3.1. Total I/VOC Emissions. Figure 2 shows the total I/VOC mass emitted per mass of paint applied (μg/g) over 48 h during the extended emission tests for each of the six paint types tested. Figure 2a shows the total emission split among VOCs and IVOCs, and Figure 2b shows emissions by the compound class.

The total I/VOC emissions varied by several orders of magnitude across the tested paint types. I/VOCs emitted from the low-gloss, indoor, water-based paints (Flat, SemiInt, and Satin) range from ∼350 to 470 μg/g of paint applied. The higher gloss, water-based paints had emissions 1−2 orders of magnitude larger than the those of low-gloss paints. High Gloss I/VOC emissions were 20 times larger than Flat paint emissions (∼7000 μg/g), and SemiExt emissions (24 000 μg/g) were a factor of 67 larger than Flat paint emissions. The oil-based paint had the highest emissions (∼2.5×10^5 μg/g).

Variations in emissions by the paint type were significantly larger than variations due to the substrate (drywall, wood, or metal) or the choice of the flux chamber (aluminum vs fiberglass). For example, substrate effects (Table S2) were ∼10−20%, similar to experiment-to-experiment variability for drywall experiments. In contrast, differences in emissions between paint classes were an order of magnitude or more (Figure 2).

This large variation in emissions indicates that representing paint I/VOC emissions in chemical transport models will require information on both the total mass of the paint used and the types of paints used. Our data indicates that emission inventories should incorporate information on three categories of paints: (1) low-gloss water-based paints, (2) high-gloss water-based paints, and (3) oil-based paints.

Our emission measurements are broadly consistent with the measurements by Stockwell et al.[23] They measured emissions from several paints and an oil-based stain using time-of-flight PTR-MS. As is the case in Figure 2, the measurements of Stockwell et al. can be binned into three classes: the oil-based stain had the highest emission (4.95×10^5 μg/g), latex paint of the unspecified gloss level had significantly lower emission (43 000 μg/g), and a low-odor "zero VOC" paint had the lowest emission (710 μg/g). The emission factors measured by Stockwell et al. are around two times higher than the measurements shown in Figure 2. This may be due to differences in either the formulation or manufacturer of the selected paints (e.g., Stockwell et al. tested an oil-based stain, while we tested an oil-based paint) or differences in sensitivity of their time-of-flight PTR-MS versus our quadrupole PTR-MS. Nonetheless, the results of Stockwell et al. show the same trend that emissions from different paints and coating classes are separated by an order of magnitude or more.

The distribution of IVOC versus VOC emissions varies by the paint type. The emissions from the lower gloss, indoor paints are almost entirely VOCs (97% on a mass basis), whereas IVOCs dominate the mass emissions from the High Gloss (91% IVOCs) and SemiExt (83% IVOCs) paints. Furthermore, as we describe in more detail below, the IVOC emissions from the lower gloss, indoor paints are small and fall below our detection limits after the first hour following paint application. This implies that emissions from the lower-gloss, indoor paints have little impact on outdoor IVOC concentrations and perhaps SOA formation.

By contrast, the high IVOC content of High Gloss and SemiExt emissions indicates that they have larger SOA formation potential. In addition, since the SemiExt paints are exterior paints, this means that 100% of their I/VOC emissions are released into the outdoor environment and therefore impact ambient I/VOC concentrations and SOA formation.

The oil-based paints have a closer to even split between IVOC and VOC emissions (39 and 61% respectively). The total I/VOC emissions from oil-based paints are about a factor of 10 larger than emissions from SemiExt, and the oil-based paint has the largest emissions of IVOCs among the paints tested here. Oil-based paints are primarily used outdoors due to their hard-wearing properties. Therefore, oil-based paints may also contribute significantly to ambient SOA formation.

Figure 2b shows that the distribution of compound classes emitted varies by the paint type. The three low-emitting low-gloss paints had a significant fraction of alcohols and ketones in their emissions. These compound classes were almost entirely due to emissions of two compounds: methanol and acetone. For these three paints, acetone and methanol comprised 51−65% of the total I/VOC emissions. As noted above, acetone is classified as an "exempt" VOC because of its low ozone formation potential.

The other paints had contributions from a wider array of individual components, and the major compound classes varied by the paint type. Table S5 indicates species that contributed >1% of the mass emissions measured by PTR-MS. Alkanes are a major component of the detected High Gloss and SemiExt emissions (42% of the total mass for each). Many of these alkanes were detected as the UCM on the Tenax sorbent tubes. Texanol was a major component of the emissions from High Gloss and SemiExt paints. A significant portion of emissions from the oil-based paints (17%) is aromatics. Aromatics typically have high SOA yields[51] and are

https://doi.org/10.1021/acs.est.2c02478
Environ. Sci. Technol. XXXX, XXX, XXX−XXX

likely to significantly contribute to the SOA formation potential from paints. The oil-based paint was also the only paint with detectable emissions of formaldehyde (73 ± 56 μg/g).

Figure 2b also shows the fraction of the observed paint mass loss that can be described by I/VOC emissions based on weighing the substrates prior to painting, immediately after painting, and then at 48-h intervals for up to one month (Figure S4). I/VOCs represent <5% of the total mass loss for the water-based paints. This is consistent with the composition of water-based paints. A 2005 CARB survey showed that water-based paints contained approximately 45% water by mass and 5% evaporative organics by mass.[52] Emissions from these paints are therefore mostly water vapor. Measured I/VOCs constitute a larger fraction of the mass loss from the oil-based paint (62%), as expected, based on the composition of the solvent.

3.2. Time Evolution of Emissions. One potential characteristic of VCPs is that they can serve as long-term, low-level emissions sources.[15,53] Our extended emission experiments examine how paint emissions evolved over time. We grouped the paints into two classes: "fast" emitting paints (Flat, SemiInt, Satin, and Oil) released most of their total emissions within 12 h after paining and nearly 100% of their emissions within 24 h; "slow" emitting paints (High Gloss and SemiExt) still had measurable emissions after 48 h. Figure 3 shows an example of the total emissions measured by PTR-MS for one fast-emitting and one slow-emitting paint and time-series traces of individual components. The remaining paints are shown in Figure S5. In general, the fast-emitting paints had most of their emissions as VOCs, whereas the slow-emitting paint emissions were mostly IVOCs.

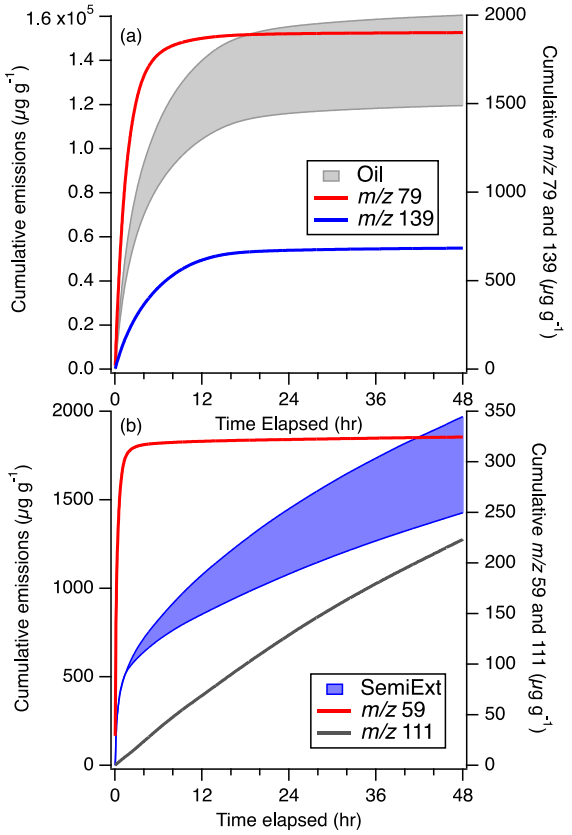

Figure 3. Cumulative emissions from (a) oil-based and (b) SemiExt paints. The colored band shows the total emissions measured by PTR-MS. The bands show the experiments with the highest and lowest total emissions. Individual traces show representative compounds (right axis).

Figure 2 shows that the organic emissions from the indoor paints (Flat, Satin, SemiInt) and the oil-based paints were primarily VOCs. Figure 3 shows that the mass emission rate from the Oil paint falls off rapidly. All four of the fast-emitting paints emit more than 80% of their total detected emissions within 12 h after application. The slow-emitting paints, such as SemiExt in Figure 2b, emitted about half of the measured emissions within 12 h and were still emitting after 48 h.

As expected, the emission profile of the paints and of representative components scales with volatility. Figure 2 shows cumulative emissions of *m/z* 79 (benzene), 139 ($C_9H_{15}O^+$), 59 (acetone), and 111 (texanol) measured by PTR-MS. Benzene (C* ~ 10^8 μg/m^3) and acetone (C* ~ 10^9 μg/m^3) are both VOCs. *M/z* 139, commonly identified as methoxy methylphenol, is a "light" IVOC (C* ~ 10^6 μg/m^3), and texanol is a lower volatility IVOC (C* ~ 10^4 μg/m^3). The VOCs are rapidly emitted, with e-folding times of 0.09 h for acetone and 1.8 h for benzene. For the fast-emitting paints dominated by VOCs, emissions of individual VOCs are similar to the emission timescale for the entire paint. The slow-emitting paints have larger contributions from slow-emitting IVOCs, and accordingly have longer emission timescales. For example, texanol has a measured e-folding time of ~33 h for the case shown in Figure 3b.

Figure 3 shows the temporal evolution of emissions measured by PTR-MS; these measurements are mostly VOCs. Figures 4 and S6 show the corresponding measurements for Tenax tubes which primarily capture IVOCs, for the Oil and High Gloss paints.

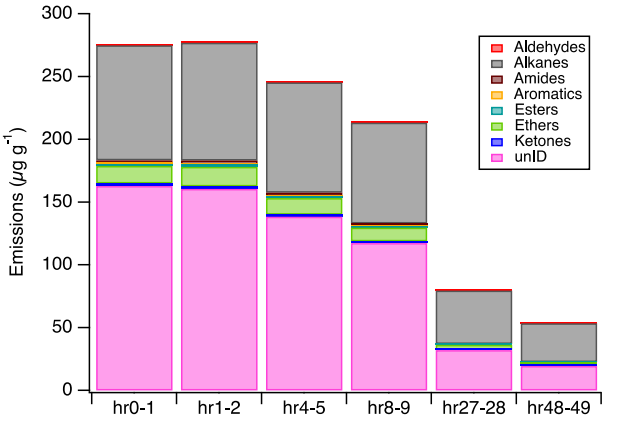

Figure 4. Extended emission samples of the High Gloss paint measured with Tenax tubes.

Figure 2 shows that the low-gloss, indoor paints (Flat, Satin, and SemiInt) all had low emissions of IVOCs. Figure S5 also shows that these paints also were "fast" emitters, with emissions measured by PTR-MS falling to zero within 24 h. The IVOCs measured with the Tenax tubes for these paints follow the same trend, and there are no long term IVOC emissions for these paints. Measurements of IVOCs using Tenax tubes were below detection limits after 1 h following paint application; the 0−1 h tubes were above the detection

https://doi.org/10.1021/acs.est.2c02478
Environ. Sci. Technol. XXXX, XXX, XXX−XXX

limit, but the 1−2 h and subsequent tubes were below the detection limit.

The two "slow" emitting paints (e.g., High Gloss in Figure 4) showed high initial IVOC emissions that decayed over time. These emissions did not reach zero over the course of the extended emission experiments. Even after 48 h, the High Gloss paint continued to emit IVOCs at 15% of the original rate during hour 0−1. The e-folding time for IVOC emissions measured on the Tenax tubes for the High Gloss paint was 25 h, similar to the 33 h e-folding time for texanol emissions from this paint. This suggests that these IVOC-dominated, slow-emitting paints maybe long-term sources of IVOCs.

The composition of IVOC emissions changed over time. For example, for the High Gloss paints, alkanes were an important component of the emissions over the entire two days, but they increased from 28% of the emitted mass during hour 0−1 to 60% at hour 47−48.

Figures 3 and 4 show that the total emissions transition from being more VOC-dominated immediately after paint application to progressively more IVOC-dominated over time. This transition is expected since the emissions seem to be mostly driven by evaporation. More volatile species will evaporate faster than lower volatility species. Nonetheless, VOC and IVOC emissions fall to zero for most of the paints tested here within 48 h of paint application.

3.3. Volatility Distributions. We used the combined PTR-MS and GC−MS data to develop volatility distributions for each of the sampled paints. Figure 5 shows the 48-h mass-weighted volatility distributions for Oil, High gloss, and Flat paints; the remaining paints are shown in Figure S7.

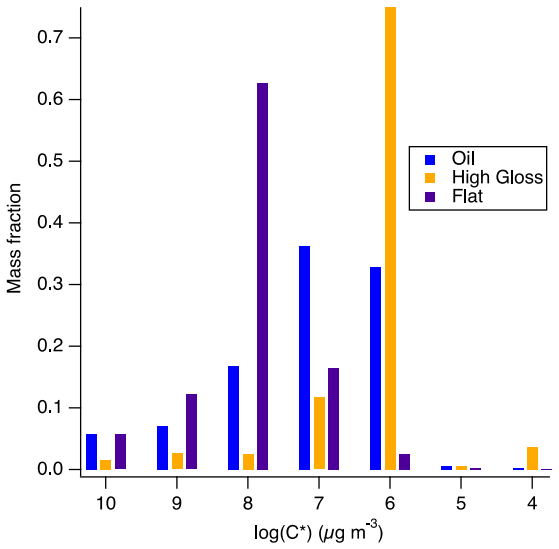

Figure 5. Mass-weighted volatility distributions for Oil, High Gloss, and Flat paints for 48 h extended emission experiments.

Emissions from the Flat paint are dominated by VOCs (Figure 2). This is evident in the volatility distribution. More than 60% of the emitted mass falls into one volatility bin ($C^* = 10^8$ $\mu g/m^3$). This is in part a consequence of the high methanol emissions, which contribute ∼60% of the total I/VOC emissions for the Flat paint. Satin and SemiInt paints (Figure S7) have similar volatility distributions with large contributions from methanol to the total I/VOC emissions.

The oil paint emissions are dominated by a broad UCM hump near the VOC/IVOC volatility border. The volatility distribution similarly peaks in the $C^* = 10^6$ and 10^7 $\mu g/m^3$ bins. Most of the emissions for the High Gloss paint are in the 10^6 $\mu g/m^3$ bin. These paints may therefore have a higher SOA formation potential than the low-gloss indoor paints.

Figure 5 shows a one-dimensional volatility distribution, where the mass is lumped only by C*. It is also common to define emissions in two-dimensional volatility space, where the second dimension is a measure of oxygenation such as the O/C molar ratio.[54] However, that is not possible in this study. Much of the mass is emitted as a broad UCM hump. While we can determine UCM volatility from GC−MS, we are not able to assign O/C or other molar markers of oxygenation without greater chemical specificity of the UCM.

3.4. Implications for SOA Formation. Here, we combine our new emission data with paint usage and literature SOA yields to estimate the total I/VOC emissions and SOA formation potential from architectural coatings. These estimates rely critically on estimates of the oil paint usage because emission factors from oil-based paints (Figure 2) are 1−3 orders of magnitude larger than those for other paint types. We explore this sensitivity by constructing three estimates of oil paint usage in this section, as shown in Figure 6.

We estimate the total architectural coating usage in the U.S. using the U.S. Economic Census to scale our measured I/VOC emission factors to the national scale.[33] This census estimated the total architectural coating usage (product code 3255101) of 651.6 million gallons in 2010. We converted this usage to mass, assuming a density of 10 pounds per gallon[52] and adjusted by population to estimate the total usage in 2021. All three of our emission estimates use the same total paint consumption (3.13×10^9 kg, or ∼10 kg per person) along with the cumulative I/VOC emissions after 48 h for each of the tested paint types.

We then construct three estimates with varying levels of the oil paint usage. The first ("Census" in Figure 6) apportions paint types to one of the six classes tested here using their 10-digit product code from the Economic Census. This apportionment is shown in Table S6 in the Supporting Information. The Census case attributes 28% of the total paint usage to oil paints.

CARB also maintains an inventory of paint and coating usage in California (https://ww2.arb.ca.gov/sites/default/files/2020-11/t3_t8_jan42018_remediated.pdf). It estimated that in 2014, solvent-borne coatings represented 6% of paint usage. We built two additional emission estimates based on this lower amount of oil paint usage. "CARB low" assumes that the remaining 94% of paints have emissions described by the mean emissions from the low-gloss, low-emitting latex paints (Flat, SemiInt, and Satin). "CARB high" assumes that the remaining paints have emissions equal to the mean emissions of the high-emitting High Gloss and SemiExt paints.

Figure 6a shows the annual I/VOC emissions for the three cases. The estimates range from 48 Gg for the CARB low case to 155 Gg for the Census case. This variation is largely driven by the differences in the oil paint usage across the three cases. We estimate I/VOC emissions of 0.15−0.48 kg/person and 15−49 g/kg of paint used. This is slightly lower than a recent inventory by Seltzer et al. (0.67 kg/person per year)[20] and significantly smaller than the estimate from McDonald et al. (1.2 Tg I/VOC emissions from architectural coatings, 3.8 kg/person/year).[14]

https://doi.org/10.1021/acs.est.2c02478
Environ. Sci. Technol. XXXX, XXX, XXX−XXX

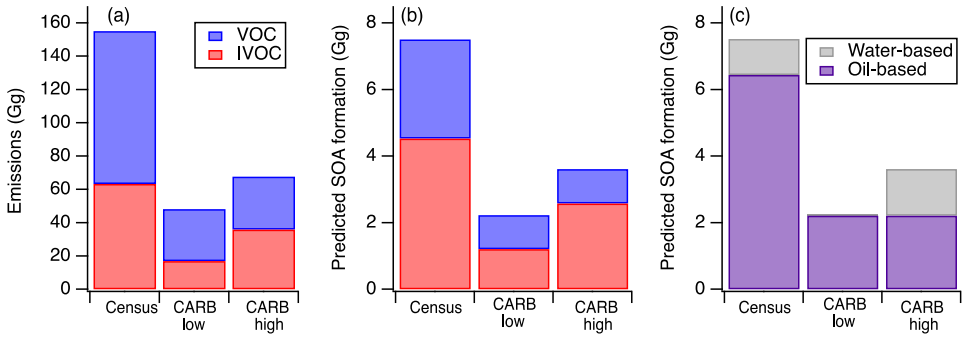

Figure 6. Annual I/VOC emissions and SOA formation from architectural coatings. (a) Total I/VOC emissions for the three sensitivity cases described in the text. (b) and (c) show predicted SOA formation, with (b) showing the contributions of VOC and IVOC to SOA formation and (c) showing contributions of oil-based versus water-based paints.

The VOC/IVOC split varies across the three cases shown in Figure 6a. The IVOC fraction ranges from 35% in the CARB low case, where the bulk of the paint mass is assumed to be VOC-dominated low-gloss paints, to 48% in the Census case.

We estimated the contribution of paint-emitted I/VOCs to ambient SOA production. We estimated SOA production by multiplying the total I/VOC emissions by SOA mass yields for each compound class. The SOA yields (g/g) were calculated using the statistical oxidation model (SOM)[55] and are shown in Table S7. These are the same SOA yields previously used by McDonald et al. to estimate the contributions of VCPs to SOA formation in Los Angeles.[14]

Figure 6b,c shows the estimated annual SOA production, which ranges from 2.2 to 7.5 Gg. As with the emission estimates, differences in predicted SOA production are primarily the result of differences in oil-based paint usage, with a smaller influence from the abundance of IVOC emissions in the two CARB cases. Oil-based paints dominate SOA formation in all the cases; oil paints (Figure 6c) are responsible for 61% (CARB high) to 99% (CARB low) of the predicted SOA mass. Thus, while oil-based paints make up a minority of the total architectural coating use, further reducing their use is the most efficient way to reduce both I/VOC emissions and SOA formation from this sector.

While IVOCs make up a minority of the emissions (Figure 6a) for all three cases, they contribute the most to the SOA formation. This is because IVOCs, which have a lower volatility than VOCs, typically have higher SOA mass yields.

To put the SOA production from paints in context, we compare it to estimates of SOA formation from vehicle emissions. Jathar et al. estimated that on-road gasoline and diesel vehicle emissions generate ~120 Gg of SOA annually in the U.S.[16] Our estimate of 2.2−7.5 Gg of SOA from paints is about 2−6% of the amount of vehicle-generated SOA. However, architectural coatings are just one component of the larger VCP sector. Thus, these calculations highlight how important it is to understand SOA formation from the entire VCP sector especially as on-road sources become cleaner and emit less SOA precursors.

There are several potential sources of uncertainty in our estimates of I/VOC emissions and subsequent SOA formation. These include uncertainty in SOA yields, especially for UCM and oxygenated VOCs that have not been directly measured in the laboratory. There may be significant variation in the paint emission rate and composition across manufacturers that we did not capture here. Since our results suggest that emissions and SOA formation are dominated by paints that are often used outdoors, the role of sunlight-driven changes in emissions[56] should be considered in future studies.

In this study, we have been able to reduce one potential source of uncertainty in the contribution of architectural coatings to ambient SOA. Three paint types that are often used indoors (Satin, SemiInt, and Flat) all had low emissions and negligible SOA contributions. One potential confounder for the ambient impact of these emissions is indoor-to-outdoor transit (i.e., paint fumes need to leave the building without being lost to walls or other surfaces). Our data suggest that these indoor paints are a minor contributor to I/VOC emissions from the paint and coating sector, and that emissions and SOA formation are dominated by oil paints used outdoors.

■ ASSOCIATED CONTENT

Supporting Information

The Supporting Information is available free of charge at https://pubs.acs.org/doi/10.1021/acs.est.2c02478.

Additional description of experimental procedures and experimental setups; specific experiments and sampling times; lists of ion identification in PTR-MS and marker ions used in GC−MS; SOA yields used in the calculation of SOA formation potential; headspace samples for all paint types; and volatility distributions for all paint types (PDF)

■ AUTHOR INFORMATION

Corresponding Author

Albert A. Presto − *Center for Atmospheric Particle Studies and Department of Mechanical Engineering, Carnegie Mellon University, Pittsburgh, Pennsylvania 15213, United States;* orcid.org/0000-0002-9156-1094; Email: apresto@andrew.cmu.edu

Authors

Rebecca Tanzer-Gruener − *Center for Atmospheric Particle Studies and Department of Mechanical Engineering, Carnegie Mellon University, Pittsburgh, Pennsylvania 15213, United States;* orcid.org/0000-0001-8994-4814

Pavithra Ethi Rajan − *Center for Atmospheric Particle Studies and Department of Mechanical Engineering, Carnegie Mellon University, Pittsburgh, Pennsylvania 15213, United States*

Liam D. Dugan − *Department of Chemistry, Carnegie Mellon University, Pittsburgh, Pennsylvania 15213, United States;* orcid.org/0000-0001-6350-5944

https://doi.org/10.1021/acs.est.2c02478
Environ. Sci. Technol. XXXX, XXX, XXX−XXX

Mark E. Bier − *Department of Chemistry, Carnegie Mellon University, Pittsburgh, Pennsylvania 15213, United States;* orcid.org/0000-0002-5220-9338

Allen L. Robinson − *Center for Atmospheric Particle Studies and Department of Mechanical Engineering, Carnegie Mellon University, Pittsburgh, Pennsylvania 15213, United States;* orcid.org/0000-0002-1819-083X

Complete contact information is available at: https://pubs.acs.org/10.1021/acs.est.2c02478

Notes

The authors declare no competing financial interest.

Experimental data are available on the KiltHub repository at the following DOI: 10.1184/R1/20288610.

■ ACKNOWLEDGMENTS

This research was funded by the U.S. National Science Foundation under grant CBET 1907446.

■ REFERENCES

(1) Di, Q.; Wang, Y.; Zanobetti, A.; Wang, Y.; Koutrakis, P.; Choirat, C.; Dominici, F.; Schwartz, J. D. Air Pollution and Mortality in the Medicare Population. *N. Engl. J. Med.* **2017**, *376*, 2513−2522.

(2) Dockery, D. W.; Pope, C. A., III; Xu, X.; Spengler, J. D.; Ware, J. H.; Fay, M. E.; Ferris, B. G.; Speizer, F. E. An Association between Air Pollution and Mortality in Six U.S. Cities. *N. Engl. J. Med.* **1993**, *329*, 1753−1759.

(3) Gakidou, E.; Afshin, A.; Abajobir, A. A.; Abate, K. H.; Abbafati, C.; Abbas, K. M.; Abd-Allah, F.; Abdulle, A. M.; Abera, S. F.; Aboyans, V.; et al. Global, Regional, and National Comparative Risk Assessment of 84 Behavioural, Environmental and Occupational, and Metabolic Risks or Clusters of Risks, 1990−2016: A Systematic Analysis for the Global Burden of Disease Study 2016. *Lancet* **2017**, *390*, 1345−1422.

(4) Zhang, Q.; Jimenez, J. L.; Canagaratna, M. R.; Allan, J. D.; Coe, H.; Ulbrich, I.; Alfarra, M. R.; Takami, A.; Middlebrook, A. M.; Sun, Y. L.; et al. Ubiquity and Dominance of Oxygenated Species in Organic Aerosols in Anthropogenically-Influenced Northern Hemisphere Midlatitudes. *Geophys. Res. Lett.* **2007**, *34*, L13801.

(5) Robinson, A. L.; Donahue, N. M.; Shrivastava, M. K.; Weitkamp, E. A.; Sage, A. M.; Grieshop, A. P.; Lane, T. E.; Pierce, J. R.; Pandis, S. N. Rethinking Organic Aerosols: Semivolatile Emissions and Photochemical Aging. *Science 80-* **2007**, *315*, 1259−1262.

(6) Volkamer, R.; Jimenez, J. L.; San Martini, F.; Dzepina, K.; Zhang, Q.; Salcedo, D.; Molina, L. T.; Worsnop, D. R.; Molina, M. J. Secondary Organic Aerosol Formation from Anthropogenic Air Pollution: Rapid and Higher than Expected. *Geophys. Res. Lett.* **2006**, *33*, L17811.

(7) Jimenez, J. L.; Canagaratna, M. R.; Donahue, N. M.; Prevot, A. S. H.; Zhang, Q.; Kroll, J. H.; DeCarlo, P. F.; Allan, J. D.; Coe, H.; Ng, N. L.; et al. Evolution of Organic Aerosols in the Atmosphere. *Science 80-* **2009**, *326*, 1525−1529.

(8) Xu, L.; Suresh, S.; Guo, H.; Weber, R. J.; Ng, N. L. Aerosol Characterization over the Southeastern United States Using High-Resolution Aerosol Mass Spectrometry: Spatial and Seasonal Variation of Aerosol Composition and Sources with a Focus on Organic Nitrates. *Atmos. Chem. Phys.* **2015**, *15*, 7307−7336.

(9) Chan, A. W. H.; Kautzman, K. E.; Chhabra, P. S.; Surratt, J. D.; Chan, M. N.; Crounse, J. D.; Kürten, A.; Wennberg, P. O.; Flagan, R. C.; Seinfeld, J. H. Secondary Organic Aerosol Formation from Photooxidation of Naphthalene and Alkylnaphthalenes: Implications for Oxidation of Intermediate Volatility Organic Compounds (IVOCs). *Atmos. Chem. Phys.* **2009**, *9*, 3049−3060.

(10) Miracolo, M. A.; Presto, A. A.; Lambe, A. T.; Hennigan, C. J.; Donahue, N. M.; Kroll, J. H.; Worsnop, D. R.; Robinson, A. L. Photo-Oxidation of Low-Volatility Organics Found in Motor Vehicle Emissions: Production and Chemical Evolution of Organic Aerosol Mass. *Environ. Sci. Technol.* **2010**, *44*, 1638−1643.

(11) Presto, A. A.; Miracolo, M. A.; Donahue, N. M.; Robinson, A. L. Secondary Organic Aerosol Formation from High-NOx Photo-Oxidation of Low Volatility Precursors: n-Alkanes. *Environ. Sci. Technol.* **2010**, *44*, 2029−2034.

(12) Zhao, Y.; Hennigan, C. J.; May, A. A.; Tkacik, D. S.; de Gouw, J. A.; Gilman, J. B.; Kuster, W. C.; Borbon, A.; Robinson, A. L. Intermediate-Volatility Organic Compounds: A Large Source of Secondary Organic Aerosol. *Environ. Sci. Technol.* **2014**, *48*, 13743−13750.

(13) Bishop, G. A.; Haugen, M. J. The Story of Ever Diminishing Vehicle Tailpipe Emissions as Observed in the Chicago, Illinois Area. *Environ. Sci. Technol.* **2018**, *52*, 7587−7593.

(14) McDonald, B. C.; de Gouw, J. A.; Gilman, J. B.; Jathar, S. H.; Akherati, A.; Cappa, C. D.; Jimenez, J. L.; Lee-Taylor, J.; Hayes, P. L.; McKeen, S. A.; et al. Volatile Chemical Products Emerging as Largest Petrochemical Source of Urban Organic Emissions. *Science 80-* **2018**, *359*, 760.

(15) Khare, P.; Gentner, D. R. Considering the Future of Anthropogenic Gas-Phase Organic Compound Emissions and the Increasing Influence of Non-Combustion Sources on Urban Air Quality. *Atmos. Chem. Phys.* **2018**, *18*, 5391−5413.

(16) Jathar, S. H.; Gordon, T. D.; Hennigan, C. J.; Pye, H. O. T.; Pouliot, G.; Adams, P. J.; Donahue, N. M.; Robinson, A. L. Unspeciated Organic Emissions from Combustion Sources and Their Influence on the Secondary Organic Aerosol Budget in the United States. *Proc. Natl. Acad. Sci. U.S.A.* **2014**, *111*, 10473−10478.

(17) Hodzic, A.; Jimenez, J. L.; Madronich, S.; Canagaratna, M. R.; DeCarlo, P. F.; Kleinman, L.; Fast, J. Modeling Organic Aerosols in a Megacity: Potential Contribution of Semi-Volatile and Intermediate Volatility Primary Organic Compounds to Secondary Organic Aerosol Formation. *Atmos. Chem. Phys.* **2010**, *10*, 5491−5514.

(18) Murphy, B. N.; Woody, M. C.; Jimenez, J. L.; Carlton, A.; Hayes, G.; Liu, P. L.; Ng, S.; Russell, N. L.; Setyan, L. M.; Xu, A.; et al. Semivolatile POA and Parameterized Total Combustion SOA in CMAQv5.2: Impacts on Source Strength and Partitioning. *Atmos. Chem. Phys.* **2017**, *17*, 11107−11133.

(19) Shah, R. U.; Coggon, M. M.; Gkatzelis, G. I.; McDonald, B. C.; Tasoglou, A.; Huber, H.; Gilman, J.; Warneke, C.; Robinson, A. L.; Presto, A. A. Urban Oxidation Flow Reactor Measurements Reveal Significant Secondary Organic Aerosol Contributions from Volatile Emissions of Emerging Importance. *Environ. Sci. Technol.* **2020**, *54*, 714−725.

(20) Seltzer, K. M.; Pennington, E.; Rao, V.; Murphy, N. B.; Isaacs, M.; Pye, K. K.; Pye, O. T. H. Reactive Organic Carbon Emissions from Volatile Chemical Products. *Atmos. Chem. Phys.* **2021**, *21*, 5079−5100.

(21) Guo, Z.; Chang, J. C. S.; Sparks, L. E.; Fortmann, R. C. Estimation of the Rate of VOC Emissions from Solvent-Based Indoor Coating Materials Based on Product Formulation. *Atmos. Environ.* **1999**, *33*, 1205−1215.

(22) Kiil, S. Drying of Latex Films and Coatings: Reconsidering the Fundamental Mechanisms. *Prog. Org. Coat.* **2006**, *57*, 236−250.

(23) Stockwell, C. E.; Coggon, M. M.; Gkatzelis, I. G.; McDonald, J.; Peischl, B. C.; Aikin, J.; Gilman, K.; Trainer, J. B.; Warneke, M.; Warneke, C. Volatile organic compound emissions from solvent- and water-borne coatings - compositional differences and tracer compound identifications. *Atmos. Chem. Phys.* **2021**, *21*, 6005−6022.

(24) Zhao, P.; Cheng, Y.-H.; Lin, C.-C.; Cheng, Y.-L. Effect of Resin Content and Substrate on the Emission of BTEX and Carbonyls from Low-VOC Water-Based Wall Paint. *Environ. Sci. Pollut. Res.* **2016**, *23*, 3799−3808.

(25) Silva, G. V.; Teresa, M.; Vasconcelos, S. D.; Santos, A. M.; Fernandes, E. O. Comparison of the Substrate Effect on VOC Emissions from Water Based Varnish and Latex Paint. *Environ. Sci. Pollut. Res.* **2003**, *10*, 209−216.

(26) Chang, J. C. S.; Tichenor, B. A.; Guo, Z.; Krebs, K. A. Substrate Effects on VOC Emissions from a Latex Paint. *Indoor Air* **1997**, *7*, 241−247.
(27) Clausen, P. A.; Wolkoff, P.; Hoist, E.; Nielsen, P. A. Long-term Emission of Volatile Organic Compounds from Waterborne Paints - Methods of Comparison. *Indoor Air* **1991**, *1*, 562−576.
(28) Lin, C.-C.; Corsi, R. L. Texanol Ester Alcohol Emissions from Latex Paints: Temporal Variations and Multi-Component Recoveries. *Atmos. Environ.* **2007**, *41*, 3225−3234.
(29) Corsi, R. L.; Lin, C.-C. Emissions of 2,2,4-Trimethyl-1,3-Pentanediol Monoisobutyrate (TMPD-MIB) from Latex Paint: A Critical Review. *Crit. Rev. Environ. Sci. Technol.* **2009**, *39*, 1052−1080.
(30) Gandolfo, A.; Marque, S.; Temime-Roussel, B.; Gemayel, R.; Wortham, H.; Truffier-Boutry, D.; Bartolomei, V.; Gligorovski, S. Unexpectedly High Levels of Organic Compounds Released by Indoor Photocatalytic Paints. *Environ. Sci. Technol.* **2018**, *52*, 11328−11337.
(31) Fortmann, R.; Roache, N.; Chang, J. C. S.; Guo, Z. Characterization of Emissions of Volatile Organic Compounds from Interior Alkyd Paint. *J. Air Waste Manage. Assoc.* **2011**, *48*, 931−940.
(32) Goliff, W. S.; Fitz, D. R.; Cocker, K.; Bumiller, K.; Bufalino, C.; Switzer, D.. Ambient Measurements of 2,2,4-Trimethyl, 1,3-Pentanediol Monoisobutyrate in Southern California. **2012**, *62*(), 680−685). DOI: 10.1080/10962247.2012.666223
(33) U.S. Census Bureau. *2012 Economic Census Survey, Manufacturing Industry Series: Materials Consumed by Kind for the U.S*, 2012.
(34) Truffier-Boutry, D.; Fiorentino, B.; Bartolomei, V.; Soulas, R.; Sicardy, O.; Benayad, A.; Damlencourt, J. F.; Pépin-Donat, B.; Lombard, C.; Gandolfo, A.; et al. Characterization of photocatalytic paints: a relationship between the photocatalytic properties - release of nanoparticles and volatile organic compounds. *Environ. Sci.: Nano* **2017**, *4*, 1998−2009.
(35) Weiss, K. D. Paint and Coatings: A Mature Industry in Transition. *Prog. Polym. Sci.* **1997**, *22*, 203−245.
(36) U.S. EPA. *National Volatile Organic Compound Emission Standards for Architectural Coatings*, 2000; p 40. CFR Part 59 Subpart D.
(37) Lindinger, W.; Hansel, A.; Jordan, A. On-Line Monitoring of Volatile Organic Compounds at Pptv Levels by Means of Proton-Transfer-Reaction Mass Spectrometry (PTR-MS) Medical Applications, Food Control and Environmental Research. *Int. J. Mass Spectrom. Ion Processes* **1998**, *173*, 191−241.
(38) Helmig, D.; Vierling, L. Water Adsorption Capacity of the Solid Adsorbents Tenax TA, Tenax GR, Carbotrap, Carbotrap C, Carbosieve SIII, and Carboxen 569 and Water Management Techniques for the Atmospheric Sampling of Volatile Organic Trace Gases. *Anal. Chem.* **2002**, *67*, 4380−4386.
(39) Maier, I.; Fieber, M. Retention Characteristics of Volatile Compounds on Tenax TA. *J. High Resolut. Chromatogr.* **1988**, *11*, 566−576.
(40) Rothweiler, H.; Wäger, P. A.; Schlatter, C. Comparison of Tenax Ta and Carbotrap for Sampling and Analysis of Volatile Organic Compounds in Air. *Atmos. Environ., Part B* **1991**, *25*, 231−235.
(41) Tkacik, D. S.; Presto, A. A.; Donahue, N. M.; Robinson, A. L. Secondary Organic Aerosol Formation from Intermediate-Volatility Organic Compounds: Cyclic, Linear, and Branched Alkanes. *Environ. Sci. Technol.* **2012**, *46*, 8773−8781.
(42) Algrim, L. B.; Ziemann, P. J. Effect of the Keto Group on Yields and Composition of Organic Aerosol Formed from OH Radical-Initiated Reactions of Ketones in the Presence of NOx. *J. Phys. Chem. A* **2016**, *120*, 6978−6989.
(43) Zhao, Y.; Nguyen, N. T.; Presto, A. A.; Hennigan, C. J.; May, A. A.; Robinson, A. L. Intermediate Volatility Organic Compound Emissions from On-Road Gasoline Vehicles and Small Off-Road Gasoline Engines. *Environ. Sci. Technol.* **2016**, *50*, 4554−4563.
(44) Zhao, Y.; Nguyen, N. T.; Presto, A. A.; Hennigan, C. J.; May, A. A.; Robinson, A. L. Intermediate Volatility Organic Compound Emissions from On-Road Diesel Vehicles: Chemical Composition, Emission Factors, and Estimated Secondary Organic Aerosol Production. *Environ. Sci. Technol.* **2015**, *49*, 11516−11526.
(45) Presto, A. A.; Hennigan, C. J.; Nguyen, N. T.; Robinson, A. L. Determination of Volatility Distributions of Primary Organic Aerosol Emissions from Internal Combustion Engines Using Thermal Desorption Gas Chromatography Mass Spectrometry. *Aerosol Sci. Technol.* **2012**, *46*, 1129−1139.
(46) Xu, R.; Alam, M. S.; Stark, C.; Harrison, R. M. Behaviour of Traffic Emitted Semi-Volatile and Intermediate Volatility Organic Compounds within the Urban Atmosphere. *Sci. Total Environ.* **2020**, *720*, 137470.
(47) Lu, Q.; Zhao, Y.; Robinson, A. L. Comprehensive Organic Emission Profiles for Gasoline, Diesel, and Gas-Turbine Engines Including Intermediate and Semi-Volatile Organic Compound Emissions. *Atmos. Chem. Phys.* **2018**, *18*, 17637−17654.
(48) Pankow, J. F.; Asher, W. E. SIMPOL.1: A Simple Group Contribution Method for Predicting Vapor Pressures and Enthalpies of Vaporization of Multifunctional Organic Compounds. *Atmos. Chem. Phys.* **2008**, *8*, 2773−2796.
(49) McLafferty, F. W.; Turecek, F. *Interpretation of Mass Spectra*, 4th ed.; University Science Books, 1993.
(50) Pagonis, D.; Sekimoto, K.; de Gouw, J. A Library of Proton-Transfer Reactions of H3O+ Ions Used for Trace Gas Detection. *J. Am. Soc. Mass Spectrom.* **2019**, *30*, 1330−1335.
(51) Akherati, A.; He, Y.; Coggon, M. M.; Koss, A.; Hodshire, A.; Sekimoto, K.; Warneke, C.; de Gouw, J. A.; Yee, L. D.; Seinfeld, J. H.; et al. Oxygenated Aromatic Compounds Are Important Precursors of Secondary Organic Aerosol in Biomass Burning Emissions. *Environ. Sci. Technol.* **2020**, *54*, 8568−8579.
(52) Davis, M. S. *2005 Architectural Coatings Survey Final Report*, 2007.
(53) Drozd, G. T.; Weber, R. J.; Goldstein, A. H. Highly Resolved Composition during Diesel Evaporation with Modeled Ozone and Secondary Aerosol Formation: Insights into Pollutant Formation from Evaporative Intermediate Volatility Organic Compound Sources. *Environ. Sci. Technol.* **2021**, *55*, 5742−5751.
(54) Donahue, N. M.; Epstein, S. A.; Pandis, S. N.; Robinson, A. L. A Two-Dimensional Volatility Basis Set: 1. Organic-Aerosol Mixing Thermodynamics. *Atmos. Chem. Phys.* **2011**, *11*, 3303−3318.
(55) Cappa, C. D.; Wilson, K. R. Multi-Generation Gas-Phase Oxidation, Equilibrium Partitioning, and the Formation and Evolution of Secondary Organic Aerosol. *Atmos. Chem. Phys.* **2012**, *12*, 9505−9528.
(56) Khare, P.; Machesky, J.; Soto, R.; He, M.; Presto, A. A.; Gentner, D. R. Asphalt-Related Emissions Are a Major Missing Nontraditional Source of Secondary Organic Aerosol Precursors. *Sci. Adv.* **2020**, *6*, No. eabb9785.

https://doi.org/10.1021/acs.est.2c02478
Environ. Sci. Technol. XXXX, XXX, XXX−XXX